Robotica (2010) volume 28, pp. 1–10. © Cambridge University Press 2009
doi:10.1017/S0263574709005475

Kinematic synthesis of tendon-driven robotic manipulators using singular value decomposition

Jinn-Biau Sheu, Jyun-Jheng Huang and Jyh-Jone Lee*

Department of Mechanical Engineering, National Taiwan University, Taipei 106, Taiwan

(Received in Final Form: February 10, 2009. First published online: March 11, 2009)

SUMMARY

This work describes a systematic methodology for the synthesis of tendon-driven manipulators. A method for enumerating the topology of tendon routings is first established. To conform with the enumerated structures, the kinematic synthesis of the manipulator using singular value decomposition is then developed. Design equations for synthesizing a general tendon-driven manipulator with isotropic transmission characteristics are subsequently derived. It is shown that the design methodology may give designers wider selection in determining the tendon routing topology than prior methods by other literature.

KEYWORDS: Tendon-driven manipulator; Singular value decomposition; Structure matrix; Isotropic transmission; Design.

1. Introduction

For a few decades, tendons have been widely used for motion and force transmission in the robotic manipulators. The main merit for using such device is that tendons allow driving actuators to be tele-operated from the system and therefore make the system lightweight and compact design feasible. However, certain disadvantages such as friction in tendon conduit, compliance, and antagonism in tendons tension may also be induced from using tendon transmission. These effects inevitably increase the complexity in designing the tendon-driven robotic system. In order to realize the characteristics of tendon-driven manipulators, a lot of research has been performed from many aspects. To name a few, the kinematics and statics of articulated tendon-driven robotics mechanisms were investigated by Morecki *et al.*,[1] Salisbury,[2] and Tsai and Lee.[3] Controls of the tendon-driven manipulators were researched by Jacobsen *et al.*,[4] Hollars and Cannon,[5] and Oh *et al.*,[6] Dynamic analysis of tendon-driven manipulators was studied by Lee and Lee,[7] Prisco and Bergamasco,[8] Voglewede and Ebert-Uphoff,[9] Barrette and Gosselin,[10] and Diao and Ma.[11] Even recently, some new technology in materials as electroactive polymers (EAP) has been proposed to emulate natural muscles and applied in the tendon-driven manipulators.[12] This emerging technology can be potentially used to make the robot without the need for traditional mechanical component as bearings, pulleys, and rotary motors. The above results provide much profound insight into the design of tendon-driven manipulators.

In order to enhance the design of tendon-driven manipulators, Lee and Tsai[13] proposed a methodology for enumerating the topology of tendon routings. Certain admissible tendon routings were obtained. Their approach was based on the assumption that all the actuators were installed on the base link and the outcome was limited to the generation of the kinematic structures with pseudo-triangular form. On the other hand, many researchers use force ellipsoids as a tool to measure the manipulability of robotic manipulators.[14,15] Lee and Tsai[16] applied this concept to the force transmission performance between joint space and tendon space of the tendon-driven manipulator. Ou and Tsai[17] further extended the concept to study the force performance between end-effector space and tendon space. They subsequently developed the methodology for the kinematic synthesis of tendon-driven manipulators with isotropic transmission characteristics. Chen *et al.*[18] used QR factorization to allow more choices in determining the pulley sizes of the tendon-driven manipulator to achieve isotropic transmission characteristics. Both works achieved some results in designing the tendon-driven manipulator with better force transmission. Nonetheless, they were limited to certain tendon routing topology and specifically applicable to the n-degree-of-freedom (DOF) tendon-driven manipulators with $(n + 1)$ tendons.

In this paper, it is our objective to synthesize the tendon-driven manipulators with general structure matrix, that is, an n-DOF system with m $(m \geq n + 1)$ tendons. First, we allow the tendon to connect between any two links of the manipulator and seek for the admissible kinematic structures. This also expands the scope of Lee and Tsai[13] to a general condition. With the enumeration results, a method using singular value decomposition (SVD) for the structure matrix is applied for the synthesis of the tendon-driven manipulators having isotropic transmission characteristics. Then, two tendon-driven manipulators of general structure will be used to demonstrate the procedure. Finally, the force transmission among various tendon routings will be compared to show their performance.

2. Principle of Operation

It has been shown by Tsai and Lee[3] that the kinematic structure of a general tendon-driven manipulator can be represented by a planar schematic form from which the

* Corresponding author. E-mail: jjlee@ntu.edu.tw

https://doi.org/10.1017/S0263574709005475 Published online by Cambridge University Press

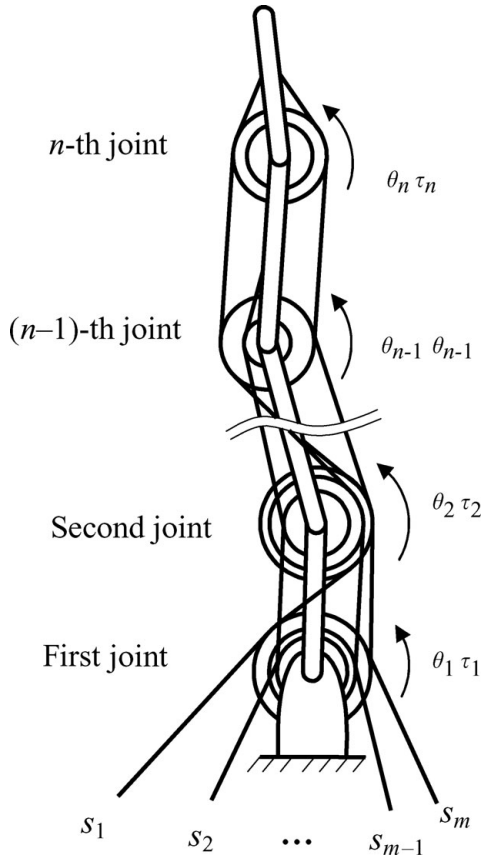


Fig. 1. A general tendon-driven manipulator.

relations between the tendon displacements and joint angles can be derived systematically. Figure 1 shows the planar schematic illustration of a general tendon-driven manipulator having n-DOF and m ($m \geq n+1$) open-end control tendons. For convenience, assume that the joints are numbered sequentially from the proximal (base) end to the distal end. The transformation from joint angles $\boldsymbol{\theta}$ to tendon linear displacements $\boldsymbol{S}$ can be written as

$$\boldsymbol{S} = \boldsymbol{A}\,\boldsymbol{\theta}, \tag{1}$$

where $\boldsymbol{S} = [s_1, s_2, \ldots, s_m]^T$ is the $(m \times 1)$ tendon displacement vector, $\boldsymbol{\theta} = [\theta_1, \theta_2, \ldots, \theta_n]^T$ is the $(n \times 1)$ joint angle vector, and $\boldsymbol{A} = [a_{ij}]$ is the $(m \times n)$ displacement structure matrix. Similarly, the transformation from tendon forces to joint torques can be written as

$$\boldsymbol{\tau} = B\,\boldsymbol{\xi}, \tag{2}$$

where $\boldsymbol{\tau} = [\tau_1, \tau_2, \ldots, \tau_n]^T$ is the $(n \times 1)$ joint torque vector, $\boldsymbol{\xi} = [\xi_1, \xi_2, \ldots, \xi_m]^T$ is the $(m \times 1)$ tendon force vector, and $\boldsymbol{B} = \boldsymbol{A}^T$ is the $(n \times m)$ force structure matrix. The element b_{ij} of $\boldsymbol{B}$ also indicates the condition of adjacency of the tendon j with joint i. The value of b_{ij} is nonzero if tendon j passes through joint i, otherwise it is zero. As mentioned by earlier researchers (Morecki,[1] Salisbury[2]), the control of an n-DOF manipulator requires at least $(n+1)$ tendons. Tsai[19] further extended the characteristics of the structure matrix $\boldsymbol{B}$ to a general n-DOF system with m ($m \geq n+1$) tendons as the following descriptions:

1. The rank of the structure matrix $\boldsymbol{B}$ must be equal to the degrees of freedom of the manipulator.
2. At least one vector in which all elements are of the same sign can be composed of from the null space of $\boldsymbol{B}$.
3. Since tendons are assumed to route from joint to joint, nonzero elements in each column of $\boldsymbol{B}$ must be consecutive.
4. There is a minimum of two nonzero elements and one sign change between elements in each row. This condition guarantees every joint can be manipulated in both directions.

Conditions 1 and 2 ensure that the manipulator is able to be controlled by the m open-end tendons, while Conditions 3 and 4 imply the adjacency condition of the tendon routing topology in an articulated robot manipulator. Equations (1) and (2) are the basic equations for the kinematics and force control of open-end tendon-driven manipulators. In the kinematic domain, once the joint angles are prescribed, linear displacements of tendons are uniquely determined. Inversely, linear displacements of tendons cannot be specified independently and must be contained in the n-dimensional column space of $\boldsymbol{A}$. In the force domain, once the tendon forces are given, the joint torques are uniquely determined. Inversely, given the joint torques, the tendon forces can be determined by the equation

$$\boldsymbol{\xi} = (\boldsymbol{B})^{+}\boldsymbol{\tau} + \boldsymbol{H}\lambda, \tag{3}$$

where $(\boldsymbol{B})^{+} = (\boldsymbol{B}^T)[\boldsymbol{B}\boldsymbol{B}^T]^{-1}$ is the pseudo-inverse of $\boldsymbol{B}$, $\boldsymbol{H}$ is an $m \times (m-n)$-dimensional matrix whose column vectors span the null space of matrix $\boldsymbol{B}$, and λ is an $(m-n) \times 1$ vector whose elements are arbitrary constants. The first item on the right-hand side of Eq. (3) is known as the particular solution while the second term is the homogeneous solution. The homogeneous solution is used to adjust the tension in tendons and hence must allow all tendons to remain in position tension.

The structure matrix $\boldsymbol{B}$ is of primary importance in determining the characteristics of a tendon-driven manipulator. Before synthesizing the dimension of the structure matrix $\boldsymbol{B}$, it is necessary to enumerate the feasible structures of a general system, i.e. an n-DOF system with $m(m \geq n+1)$ tendons. Without loss of generality, we assume that each tendon can route between any two links.

Let m_i be the number of tendons in a group in which every tendon is incident with i joints. Thus, the total number of tendons in all possible groups will be equal to m. We have

$$\sum_{i=1}^{n} m_i = i. \tag{4}$$

The maximal times that all tendons are incident with the joints occur at the condition when all tendons are attached to the distal link and route down to the base link. This number constitutes the upper limit of the possible incidence of tendons and joints. Therefore, the following inequality

https://doi.org/10.1017/S0263574709005475 Published online by Cambridge University Press

Table I. Feasible structure matrices for two-DOF system with four tendons, "# " denotes nonzero element.

(m_1, m_2)	Types of structure matrix
(0, 4)	$\begin{bmatrix} \# & \# & \# & \# \\ \# & \# & \# & \# \end{bmatrix}$
(1, 3)	$\begin{bmatrix} \# & \# & \# & \# \\ \# & \# & \# & 0 \end{bmatrix} \begin{bmatrix} \# & \# & \# & 0 \\ \# & \# & \# & \# \end{bmatrix}$
(2, 2)	$\begin{bmatrix} \# & \# & \# & \# \\ \# & \# & 0 & 0 \end{bmatrix} \begin{bmatrix} \# & \# & \# & 0 \\ \# & \# & 0 & \# \end{bmatrix} \begin{bmatrix} \# & \# & 0 & 0 \\ \# & \# & \# & \# \end{bmatrix}$
(3, 1)	$\begin{bmatrix} \# & \# & \# & 0 \\ \# & 0 & 0 & \# \end{bmatrix} \begin{bmatrix} \# & \# & 0 & 0 \\ \# & 0 & \# & \# \end{bmatrix}$
(4, 0)	$\begin{bmatrix} \# & \# & 0 & 0 \\ 0 & 0 & \# & \# \end{bmatrix}$

holds:

$$m_1 + 2m_2 + 3m_3 + \cdots + nm_n \leq nm. \tag{5}$$

On the other hand, the minimal times that all tendons are incident with the joints can be established using the fact that the system is controllable when each joint is at most controlled by two tendons. This may yield two conditions: if m is less than or equal to $2n$, then the number is $2n$; otherwise it is m. Therefore, the lower limit of the times that the tendons are incident with the joints will be

$$m_1 + 2m_2 + 3m_3 + \cdots + nm_n \geq 2n. \tag{6}$$

Applying Eqs. (4)–(6) and Conditions 3 and 4 as the constraints, all possible topological structures for n-DOF tendon-driven manipulators with m tendons can be enumerated. For example, if the structure of a two-DOF manipulator with four tendons is to be enumerated, writing Eqs. (4)–(6) for $n = 2$ and $m = 4$, yields

$$m_1 + m_2 = 4$$

$$m_1 + 2m_2 \leq 8$$

$$m_1 + 2m_2 \geq 4$$

Solving the above equations for m_1 and m_2, (m_1, m_2) can be obtained as (0, 4) or (1, 3) or (2, 2) or (3, 1) or (4, 0). Table I shows the feasible structure matrices corresponding to the above possible solutions. In the table, sign "#" denotes a nonzero element. Similarly, if the structure of a three-DOF manipulator with five tendons is to be synthesized, one can write $n = 3$, $m = 5$ and the possible solutions, (m_1, m_2, m_3), can be obtained as (0, 0, 5), (0, 1, 4), (1, 0, 4), (0, 2, 3), (1, 1, 3), (2, 0, 3), (0, 3, 2), (1, 2, 2), (2, 1, 2), (3, 0, 2), (0, 4, 1), (1, 3, 1), (2, 2, 1), (3, 1, 1), (4, 0, 1), (0, 5, 0), (1, 4, 0), (2, 3, 0), (3, 2, 0), and (4, 1, 0). There are a total of 117 feasible structures corresponding to the above possible solutions. For detailed results refer to ref. [20]. Table II shows two solution sets and the corresponding feasible structures in which some will be used for dimensional synthesis of the structure matrix in the later section.

Table II. Some feasible structure matrices for three-DOF system with five tendons, "# " denotes nonzero element.

(m_1, m_2, m_3)	Types of structure matrix
(0, 1, 4)	$\begin{bmatrix} \# & \# & \# & \# & \# \\ \# & \# & \# & \# & \# \\ \# & \# & \# & \# & 0 \end{bmatrix} \begin{bmatrix} \# & \# & \# & \# & 0 \\ \# & \# & \# & \# & \# \\ \# & \# & \# & \# & \# \end{bmatrix}$
(2, 1, 2)	$\begin{bmatrix} \# & \# & \# & \# & \# \\ \# & \# & \# & 0 & 0 \\ \# & \# & 0 & 0 & 0 \end{bmatrix} \begin{bmatrix} \# & \# & \# & \# & 0 \\ \# & \# & \# & 0 & \# \\ \# & \# & 0 & 0 & 0 \end{bmatrix} \begin{bmatrix} \# & \# & \# & \# & 0 \\ \# & \# & \# & 0 & 0 \\ \# & \# & 0 & 0 & \# \end{bmatrix}$ $\begin{bmatrix} \# & \# & \# & 0 & 0 \\ \# & \# & \# & \# & \# \\ \# & \# & 0 & 0 & 0 \end{bmatrix} \begin{bmatrix} \# & \# & \# & 0 & 0 \\ \# & \# & \# & \# & 0 \\ \# & \# & 0 & 0 & \# \end{bmatrix} \begin{bmatrix} \# & \# & \# & 0 & 0 \\ \# & \# & \# & 0 & \# \\ \# & \# & 0 & \# & \# \end{bmatrix}$ $\begin{bmatrix} \# & \# & 0 & \# & \# \\ \# & \# & \# & 0 & 0 \\ \# & \# & \# & 0 & 0 \end{bmatrix} \begin{bmatrix} \# & \# & 0 & \# & 0 \\ \# & \# & \# & 0 & \# \\ \# & \# & \# & 0 & 0 \end{bmatrix} \begin{bmatrix} \# & \# & 0 & \# & 0 \\ \# & \# & \# & 0 & 0 \\ \# & \# & \# & 0 & \# \end{bmatrix}$ $\begin{bmatrix} \# & \# & 0 & 0 & 0 \\ \# & \# & \# & \# & \# \\ \# & \# & \# & 0 & 0 \end{bmatrix} \begin{bmatrix} \# & \# & 0 & 0 & 0 \\ \# & \# & \# & \# & 0 \\ \# & \# & \# & 0 & \# \end{bmatrix} \begin{bmatrix} \# & \# & 0 & 0 & 0 \\ \# & \# & \# & 0 & 0 \\ \# & \# & \# & \# & \# \end{bmatrix}$

3. Isotropic Transmission

A tendon-driven manipulator that possesses isotropic transmission characteristics may even have more force distribution during the operation. Ou and Tsai[17] defined the following two conditions for a manipulator to have isotropic transmission characteristics:

$$\text{cond}(\boldsymbol{B}^+ \boldsymbol{J}^T) = 1, \tag{7}$$

$$\boldsymbol{B}\,\boldsymbol{\xi}_{\text{h}} = 0, \tag{8}$$

where cond$(\cdot)$ denotes the condition number of $(\cdot)$ and the value is the ratio of maximum singular value to minimum singular value of $(\cdot)$, $\boldsymbol{B}^+$ is the pseudo-inverse of $\boldsymbol{B}$, $\boldsymbol{J}$ is the Jacobian matrix of the manipulator, and $\boldsymbol{\xi}_h = [1, 1, \ldots, 1]^T$ is an $(m \times 1)$ isotropic vector. Mathematically, the product of $(\boldsymbol{B}^+ \boldsymbol{J}^T)$ and the force applied on the end-effector serves as the particular solution for the tendon tension while its condition number measures the shape of the ellipsoid formed by the row vector space of $(\boldsymbol{B}^+ \boldsymbol{J}^T)$. The isotropic vector $\boldsymbol{\xi}_h$ is the homogeneous solution to tendon forces that results in no net joint torques and can provide a uniform force increase in all tendons from being slack. As a result in Ou and Tsai,[17] Eq. (7) was deduced to

$$\boldsymbol{B}\boldsymbol{B}^T = \frac{1}{c_1^2} \boldsymbol{J}^T \boldsymbol{J}, \tag{9}$$

where c_1 is a nonzero constant. Equations (8) and (9) can be used to derive equations for the synthesis of tendon-driven manipulators with isotropic transmission characteristics. In what follows, we shall apply SVD method to synthesize the structure matrix $\boldsymbol{B}$. The advantage of using SVD lies in that the procedure provides a systematic decomposition of the kinematic structure and the singular values can be directly used for the force transmission evaluation. Let the SVD of a matrix $\boldsymbol{B}$ be expressed as

$$\boldsymbol{B} = \boldsymbol{U}\,\boldsymbol{D}\,\boldsymbol{V}^{\boldsymbol{T}} \tag{10a}$$

https://doi.org/10.1017/S0263574709005475 Published online by Cambridge University Press

where $\boldsymbol{U}$ is an $(n \times n)$ unitary matrix, $\boldsymbol{V}$ is an $(m \times m)$ unitary matrix, and the singular matrix $\boldsymbol{D}$ is

$$\boldsymbol{D} = \begin{bmatrix} d_1 & 0 & \cdots & 0 & \cdots & 0 \\ 0 & d_2 & \cdots & 0 & \cdots & 0 \\ \vdots & \vdots & \ddots & \vdots & \vdots & \vdots \\ 0 & 0 & \cdots & d_n & \cdots & 0 \end{bmatrix}_{n \times m} \tag{10b}$$

and where singular values $d_1 \geq d_2 \geq \cdots \geq d_n \geq 0$. The SVD of $\boldsymbol{B}^+$ can be obtained by substituting Eq. (10a) into the expression $(\boldsymbol{B})^+ = (\boldsymbol{B}^T)[\boldsymbol{B}\boldsymbol{B}^T]^{-1}$ as

$$\boldsymbol{B}^+ = \boldsymbol{V}\,\boldsymbol{D}^+\boldsymbol{U}^{\boldsymbol{T}} \tag{11a}$$

and

$$(\boldsymbol{D})+ = (\boldsymbol{D}^T)[\boldsymbol{D}D^T]^{-1} = \begin{bmatrix} 1/d_1 & 0 & \cdots & 0 \\ 0 & 1/d_2 & \cdots & 0 \\ \vdots & \vdots & \ddots & \vdots \\ 0 & 0 & \cdots & 1/d_n \\ \vdots & \vdots & \vdots & \vdots \\ 0 & \cdots & \cdots & 0 \end{bmatrix}_{m \times n} \tag{11b}$$

Likewise, the SVD of the Jacobian matrix of the manipulator $\boldsymbol{J}$, can be expressed as

$$\boldsymbol{J} = \boldsymbol{P}\,\boldsymbol{\Sigma}\,\boldsymbol{Q}^{\boldsymbol{T}}, \tag{12a}$$

where $\boldsymbol{P}$ and $\boldsymbol{Q}$ are $(n \times n)$ unitary matrices, and

$$\boldsymbol{\Sigma} = \begin{bmatrix} \sigma_1 & 0 & \cdots & 0 \\ 0 & \sigma_2 & \cdots & \vdots \\ \cdots & \cdots & \ddots & \vdots \\ 0 & \cdots & 0 & \sigma_n \end{bmatrix} \tag{12b}$$

is an $(n \times n)$ diagonal matrix whose diagonal elements are the singular values. Substituting Eqs. (11a) and (12a) into Eq. (7) yields

$$\text{cond}(\boldsymbol{V}\,\boldsymbol{D}^+\boldsymbol{U}^{\boldsymbol{T}}\,\boldsymbol{Q}\,\boldsymbol{\Sigma}^{\boldsymbol{T}}\,\boldsymbol{P}^{\boldsymbol{T}}) = 1. \tag{13}$$

If $\boldsymbol{U}$ is chosen to be equal to $\boldsymbol{Q}$ and noting that $\boldsymbol{Q}$ is unitary, Eq. (13) implies that the diagonal elements in the product $(\boldsymbol{D}^+\boldsymbol{\Sigma}^T)$ must be equal to a constant value. That is

$$di = \sigma_i/c_2 \quad \text{for} \quad i = 1, 2, \ldots, n, \tag{14}$$

where c_2 is a nonzero scaling constant. Therefore, from Eqs. (10a), (12a), and (14), we can find matrices $\boldsymbol{U}$ and $\boldsymbol{D}$ of Eq. (10a) once the Jacobian matrix $\boldsymbol{J}$ of the manipulator is identified. Now, to obtain the structure matrix $\boldsymbol{B}$, it is still necessary to find the matrix $\boldsymbol{V}$. Since $\boldsymbol{V}$ is unitary, the elements $v_{ij}{}'s$ in $\boldsymbol{V}$ satisfy the orthogonality conditions

$$\sum_{j=1}^{m} v_{ji}^2 = 1 \quad \text{for} \quad i = 1, 2, \ldots, m \tag{15a}$$

and

$$\sum_{j=1}^{m} v_{ji}\,v_{jk} = 0 \quad \text{for} \quad i = 1, 2, \ldots, n; \quad k = 1, 2, \ldots, n; \; i \neq k \tag{15b}$$

The number of equations available in Eq. (15a) and (15b) is $m(m+1)/2$. Since the total unknowns in matrix $\boldsymbol{V}$ is m^2, there are $m(m-1)/2$ equations required in order to solve the unknowns elements in $\boldsymbol{V}$. It can be shown[21] that the column vectors in $\boldsymbol{V}$ can be arranged such that the first n columns contain the right singular vectors of $\boldsymbol{B}$, and the remaining columns are the eigenvectors corresponding to the zero eigenvalues of $\boldsymbol{B}^T\boldsymbol{B}$. Let the column vectors corresponding to the zero eigenvalues be $\boldsymbol{V}_{ze} = (\boldsymbol{v}_{n+1}, \ldots, \boldsymbol{v}_m)$. Then, the column vectors of $\boldsymbol{V}_{ze}$ form an orthonormal basis of null space of $\boldsymbol{B}$. Therefore,

$$\boldsymbol{B}V_{ze} = 0. \tag{16}$$

Thus, to yield isotropic transmission characteristics required by Eq. (8), $\boldsymbol{V}_{ze}$ must be able to become the vector base of isotropic vector $\boldsymbol{\xi}_h$. This condition will yield $(m-1)$ constraints. For simplicity, one of the column vectors of $\boldsymbol{V}_{ze}$ can be chosen to be equal to $\boldsymbol{\xi}_m$. For example, if the last column vector of $\boldsymbol{V}_{ze}$ is selected, then

$$v_{1,m} = v_{2,m} = v_{3,m} = \cdots = v_{m,m}. \tag{17}$$

In addition to Eqs. (15a) and (15b), Eq. (17) provides $(m-1)$ constraints. Thus, there will be $(m-1)(m-2)/2$ free choices left in determining the elements of $\boldsymbol{V}$. These free choices can be used to specify the types of routing of the tendon-driven manipulators. The procedure for determining the types of structure matrix and the dimension of the structure can be summarized as follows:

1. Determine the Jacobian matrix $\boldsymbol{J}$ of the manipulator. Then, find the SVD of $\boldsymbol{J}$ as $\boldsymbol{J} = \boldsymbol{P}\Sigma\boldsymbol{Q}^T$.
2. Let $\boldsymbol{U} = \boldsymbol{Q}$ and $\boldsymbol{D} = \boldsymbol{\Sigma}$. Substituting the results into Eq. (10a), yields

$$\boldsymbol{B} = \frac{1}{c_2} \begin{bmatrix} u_{11}d_{11}v_{11} + u_{12}d_{22}v_{12} + \cdots + u_{1n}d_{nn}v_{1n} & u_{11}d_{11}v_{21} + u_{12}d_{22}v_{22} + \cdots + u_{1n}d_{nn}v_{2n} & \cdots & \cdots & u_{11}d_{11}v_{m1} + u_{12}d_{22}v_{m2} + \cdots + u_{1n}d_{nn}v_{mn} \\ u_{21}d_{11}v_{11} + u_{22}d_{22}v_{12} + \cdots + u_{2n}d_{nn}v_{1n} & u_{21}d_{11}v_{21} + u_{22}d_{22}v_{22} + \cdots + u_{2n}d_{nn}v_{2n} & \cdots & \cdots & u_{21}d_{11}v_{m1} + u_{22}d_{22}v_{m2} + \cdots + u_{2n}d_{nn}v_{mn} \\ \vdots & \vdots & \cdots & \cdots & \vdots \\ u_{n1}d_{11}v_{11} + u_{n2}d_{22}v_{12} + \cdots + u_{nn}d_{nn}v_{1n} & u_{n1}d_{11}v_{21} + u_{n2}d_{22}v_{22} + \cdots + u_{nn}d_{nn}v_{2n} & \cdots & \cdots & u_{n1}d_{11}v_{m1} + u_{n2}d_{22}v_{m2} + \cdots + u_{nn}d_{nn}v_{mn} \end{bmatrix}. \tag{18a}$$

https://doi.org/10.1017/S0263574709005475 Published online by Cambridge University Press

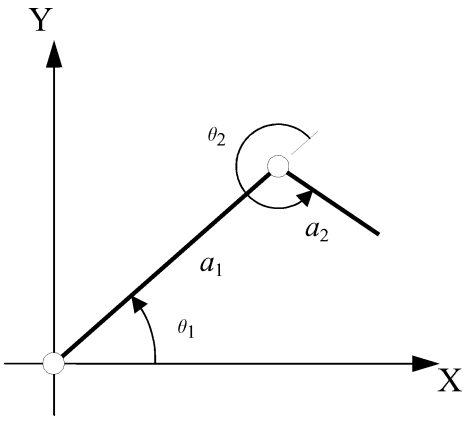


Fig. 2. A two-DOF robot manipulator system.

Or in a recursive form

$$b_{ij} = \frac{1}{c_2}\sum_{k=1}^{n} u_{ik} d_{kk} v_{jk} \quad \text{for}$$
$$i = 1, 2, \ldots, n; \quad j = 1, 2, \ldots, m. \qquad (18b)$$

3. Select a feasible type of structure matrix from Tables 1 or 2 or known atlas. Then, compare Eq. (18a) with the selected type of structure. The zero elements in the selected matrix can be regarded as the additional topology constraints besides Eqs. (15a), (15b), and (17). If there are still free choices left, then the elements can be specified according to other applicable geometric constraints.

4. Examples

4.1. Example 1: a two-DOF robotic manipulator with four tendons

A two-DOF robotic manipulator with four tendons is first selected for demonstration. This type of structure cannot be synthesized by Ou and Tsai[17] and Chen *et al.*[18]. As shown in Fig. 2, assume that the link length a_1/a_2 is 0.6/0.3 and the isotropic position to be synthesized is chosen at joint angles $\theta_1 = 60^\circ$ and $\theta_2 = 130^\circ$. The Jacobian matrix for this manipulator is given by

$$\boldsymbol{J} = \begin{bmatrix} -a_1 \sin\theta_1 - a_2 \sin(\theta_1 + \theta_2) & -a_2 \sin(\theta_1 + \theta_2) \\ a_1 \cos\theta_1 + a_2 \cos(\theta_1 + \theta_2) & a_2 \cos(\theta_1 + \theta_2) \end{bmatrix} \qquad (19)$$

After substituting the link parameters into $\boldsymbol{J}$ and applying singular value decomposition to the Jacobian at the given posture, matrices $\boldsymbol{U}$ and $\boldsymbol{D}$ can be found as

$$\boldsymbol{U} = \begin{bmatrix} 0.9820 & -0.1890 \\ -0.1890 & -0.9820 \end{bmatrix} \quad \text{and}$$
$$\boldsymbol{D} = \begin{bmatrix} 0.4728 & 0 & 0 & 0 \\ 0 & 0.2916 & 0 & 0 \end{bmatrix}.$$

Again, substituting $\boldsymbol{U}$ and $\boldsymbol{D}$ into Eq. (18a) yields

$$\boldsymbol{B} = \frac{1}{c_2}\begin{bmatrix} 0.4643v_{11} - 0.0551v_{12} & 0.4643v_{21} - 0.0551v_{22} & 0.4643v_{31} - 0.0551v_{32} & 0.4643v_{41} - 0.0551v_{42} \\ -0.0894v_{11} - 0.2864v_{12} & -0.0894v_{21} - 0.2864v_{22} & -0.0894v_{31} - 0.2864v_{32} & -0.0894v_{41} - 0.2864v_{42} \end{bmatrix} \qquad (20)$$

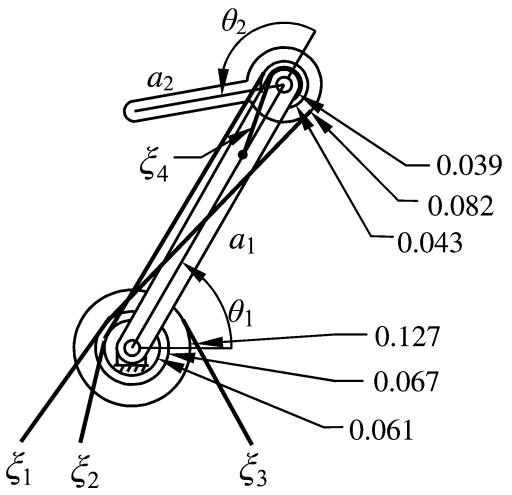


Fig. 3. Schematic illustration of the synthesized two-DOF, four-tendon system.

Since there can be three free choices in determining the elements in $\boldsymbol{B}$ for a two-DOF system with four tendons, all the kinematic structures except $(m_1, m_2) = (4, 0)$ listed in Table I can be used for designing. If the second structure of type (2, 2) is arbitrarily selected, then two equations $b_{14} = b_{23} = 0$ are set as the constraints for the structure matrix in addition to the constraints provided by Eqs. (15a), (15b), and (17). There still has one free choice, therefore, one other element can be chosen as known value, for example, let $b_{11} = 0.2$. Thus, the constraint equations are

$$v_{14} = v_{24} = v_{34} = v_{44} \qquad (21a)$$

$$0.463v_{11} - 0.0551v_{12} = 0.2 \qquad (21b)$$

$$0.4643v_{41} - 0.0551v_{42} = 0 \qquad (21c)$$

$$-0.0894v_{31} - 0.2864v_{32} = 0 \qquad (21d)$$

Solving Eqs. (21a)–(21d) along with orthogonality conditions for $v_{ij}'s$, yields

$$\boldsymbol{V} = \begin{bmatrix} 0.513 & 0.695 & -0.059 & 0.5 \\ 0.326 & -0.551 & 0.583 & 0.5 \\ -0.793 & 0.246 & 0.247 & 0.5 \\ -0.046 & -0.39 & -0.772 & 0.5 \end{bmatrix} \qquad (22)$$

or

$$\boldsymbol{B} = \boldsymbol{U}\,\boldsymbol{D}\,\boldsymbol{V}^{\boldsymbol{T}} = \frac{1}{c_2}\begin{bmatrix} 0.2 & 0.182 & -0.382 & 0 \\ -0.245 & 0.129 & 0 & 0.116 \end{bmatrix} \qquad (23)$$

Figure 3 shows the schematic diagram of the synthesized manipulator with the scaling constant $c_2 = 3$.

https://doi.org/10.1017/S0263574709005475 Published online by Cambridge University Press

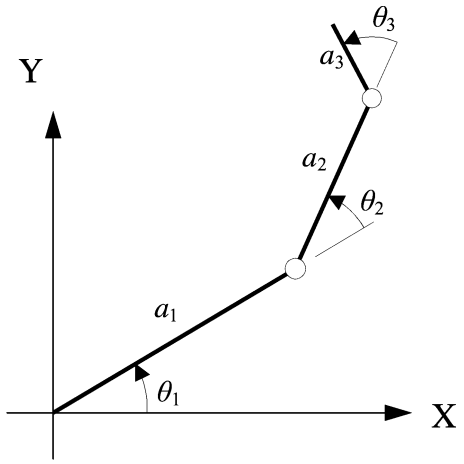


Fig. 4. A three-DOF robot manipulator system.

4.2. Example 2: a planar three-DOF robotic manipulator with five tendons

To synthesize a three-DOF system with isotropic transmission characteristic, a planar robot manipulator with five tendons is illustrated. As shown in Fig. 4, we will find the structure matrix for the system at a given posture as $a_1 = 2, a_2 = 1.6, a_3 = 1.2, \theta_1 = 30^\circ, \theta_2 = 80^\circ$, and $\theta_3 = 20^\circ$. The Jacobian matrix of this system is

$$\boldsymbol{J} = \begin{bmatrix} -a_1 \sin\theta_1 - a_2 \sin(\theta_1+\theta_2) - a_3 \sin(\theta_1+\theta_2+\theta_3) & -a_2 \sin(\theta_1+\theta_2) - a_3 \sin(\theta_1+\theta_2+\theta_3) & -a_3 \sin(\theta_1+\theta_2+\theta_3) \\ a_1 \cos\theta_1 + a_2 \cos(\theta_1+\theta_2) + a_3 \cos(\theta_1+\theta_2+\theta_3) & a_2 \cos(\theta_1+\theta_2) + a_3 \cos(\theta_1+\theta_2+\theta_3) & a_3 \cos(\theta_1+\theta_2+\theta_3) \\ 1 & 1 & 1 \end{bmatrix} \quad (24)$$

Substituting the numerical data into $\boldsymbol{J}$ and applying SVD to the matrix, matrices $\boldsymbol{U}$ and $\boldsymbol{D}$ are obtained as

$$\boldsymbol{U} = \begin{bmatrix} 0.7452 & -0.6531 & 0.1348 \\ 0.6029 & 0.5735 & -0.5547 \\ 0.285 & 0.4946 & 0.8211 \end{bmatrix} \quad \text{and}$$

$$\boldsymbol{D} = \begin{bmatrix} 4.6289 & 0 & 0 & 0 & 0 \\ 0 & 1.5189 & 0 & 0 & 0 \\ 0 & 0 & 0.4482 & 0 & 0 \end{bmatrix}$$

For a three-DOF system with five tendons, there can be six free choices in determining the structure matrix. Here, the first one of the feasible structures $(m_1, m_2, m_3) = (2, 1, 2)$ as listed in Table II is selected as the structure to be synthesized. According to the topology of the structure, $b_{24} = b_{25} = b_{33} = b_{34} = b_{35} = 0$ will automatically be the five constraints among the six free choices. If $b_{11} = 2$ is arbitrarily set as the sixth choice, the structure matrix $\boldsymbol{B}$ can be solved as

$$\boldsymbol{B} = \frac{1}{c_2} \begin{bmatrix} 2 & -1.4653 & -2.0442 & 1.5978 & -0.0883 \\ 2.3733 & -1.4693 & -0.904 & 0 & 0 \\ 1.1046 & -1.1046 & 0 & 0 & 0 \end{bmatrix} \quad (25)$$

In view of the result of $\boldsymbol{B}$, some of the pulley sizes are greater than the link length. Thus, the scaling constant c_2 can be used to adjust the pulley sizes accordingly.

5. Tendon Forces

To evaluate the force performance among different structures, we will investigate the tendon forces of the synthesized systems throughout the workspace. The static force relationship between external forces acting on the end-effector and tendon forces can be obtained by substituting $\boldsymbol{\tau} = \boldsymbol{J}^T \boldsymbol{f}$ into Eq. (3) as

$$\boldsymbol{\xi} = \boldsymbol{B}^+ \boldsymbol{J}^T \boldsymbol{f} + \lambda \boldsymbol{H}, \quad (26)$$

where $\boldsymbol{f}$ is an $(n \times 1)$ general force vector acting on the end-effector as shown in Fig. 5.

If the force vector $\boldsymbol{f}$ is confined to be bounded on a unit circle (Newton), Eq. (26) can be used to find the corresponding tendon forces. For the purpose of comparison, the value λ in Eq. (26) is adjusted such that one of the tendons has zero tendon force while the other tendons have nonnegative tensions. Also, to achieve a fair comparison among various structures, the scaling constant c_2 in matrix $\boldsymbol{B}$ is chosen to be equal to the square root of the multiplication of the singular values of $\boldsymbol{B}$. This assumption also makes the

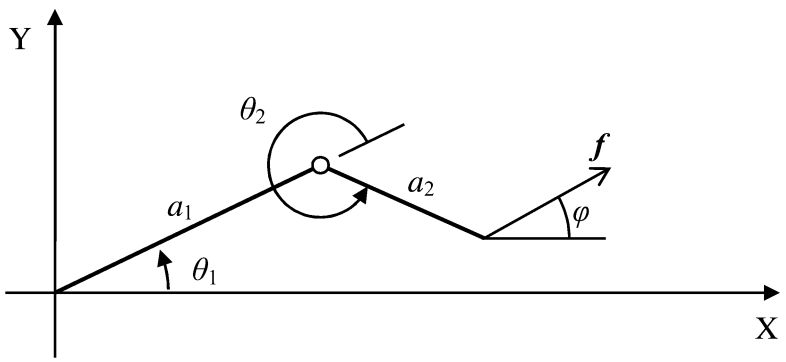


Fig. 5. General force vector $\boldsymbol{f}$ acting on a two-DOF planar manipulator.

https://doi.org/10.1017/S0263574709005475 Published online by Cambridge University Press

Table III. Four different structures for two-DOF system.

No.	Structure matrix $\boldsymbol{B}$	c_2	$\boldsymbol{H}$	Cond($\boldsymbol{B}$)
a	$\frac{1}{c_2}\begin{bmatrix} -0.2482 & -0.1270 & 0.3753 \\ 0.2121 & -0.2121 & 0 \end{bmatrix}$	0.3713	$\begin{bmatrix} 1 & 1 & 1 \end{bmatrix}^T$	1.6214
b	$\frac{1}{c_2}\begin{bmatrix} 0.5774 & 0.5774 & -1.1547 \\ 1 & -1 & 0 \end{bmatrix}$	1.4142	$\begin{bmatrix} 1 & 1 & 1 \end{bmatrix}^T$	1
c	$\frac{1}{c_2}\begin{bmatrix} 0.2 & 0.1816 & -0.3816 & 0 \\ 0.2449 & 0.1281 & 0 & 0.1167 \end{bmatrix}$	0.3713	$\begin{bmatrix} 1 & 1 & 1 & 1 \end{bmatrix}^T$	1.6212
d	$\frac{1}{c_2}\begin{bmatrix} 0.2 & 0.1816 & -0.3816 & 0 \\ 0.2453 & 0.1500 & 0.0102 & 0.0851 \end{bmatrix}$	0.3713	$\begin{bmatrix} 1 & 1 & 1 & 1 \end{bmatrix}^T$	1.6211

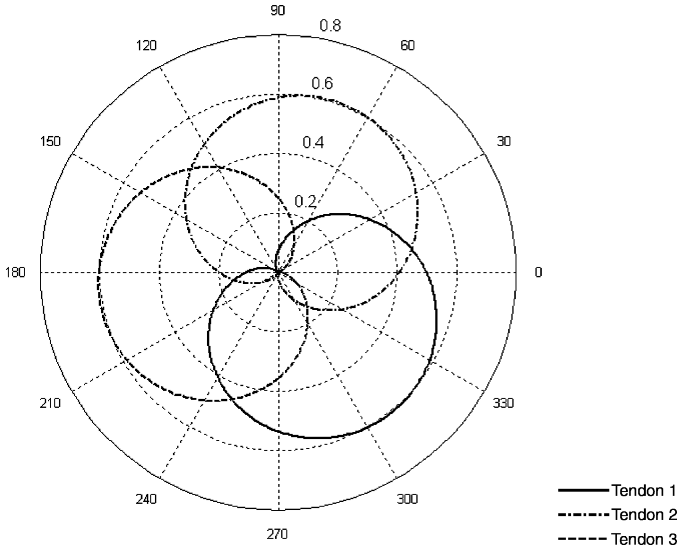


Fig. 6. Tendon forces (Newton) in structure No. (a), evaluated at isotropic posture.

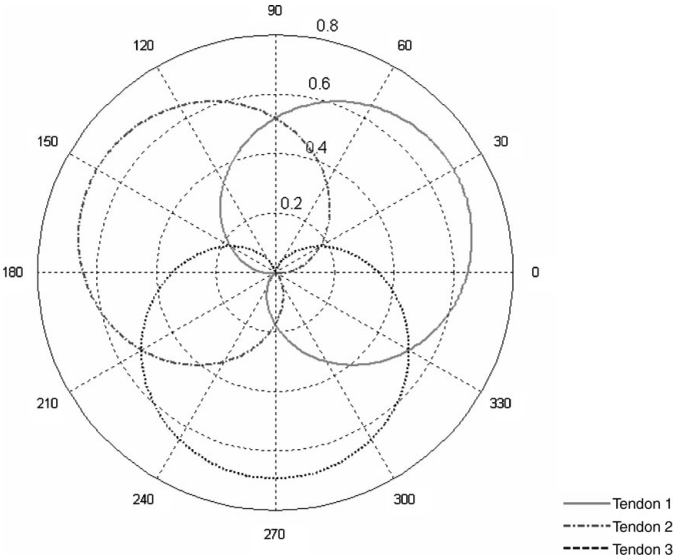


Fig. 7. Tendon forces (Newton) in structure No. (b), evaluated at isotropic posture.

area of the ellipse formed by the particular solution to be equal to the area formed by the force vector.

Table III lists four different structures and their corresponding properties. No. (a) is a two-DOF system having three tendons and isotropic transmission characteristics. The link length and joint angles are the same as those of Example 1. No. (b) is the structure matrix designed by OU and Tsai[17] whose link parameters are $a_1 = L(m)$, $a_2 = 0.707L$ (m), and the isotropic position is at joint angles $\theta_1 = 45^\circ$, $\theta_2 = 225^\circ$. In this work, we let $L = 0.6$ to make the first link to have the same length as that of the other three structures. No. (c) is the structure of Example 1. No. (d) is chosen from the first structure matrix of type (1, 3) in Table I and has the same link parameters as No. (c).

Figures 6–9 are the polar plots of the tendon tension distribution for these four structure matrices, all evaluated at their isotropic position. In these figures, the radial distance represents the magnitude of tendon force while the phase angle represents the direction of the applied force. For the two-DOF system with three tendons, Nos. (a) and (b) have similar force distribution. To find the maximal tendon forces of the structure matrix at different positions, we vary the joint angles step by step, to make links 1 and 2 rotate 360°. Then we calculate the maximal tendon forces by varying the direction of applied force at each position. Figures 10–13 show the maximal tendon tensions throughout the positions for these four structure matrices. From Figs. 6–9, the maximal tendons forces for Nos. (a) and (b) at the isotropic posture have the ratio of (1:1:1) due to the isotropic characteristics, but the ratio varies at all other positions. Thus the isotropic transmission characteristic remains valid only at the isotropic posture. Table IV shows the comparison of the maximum tendon forces at the isotropic posture and throughout the

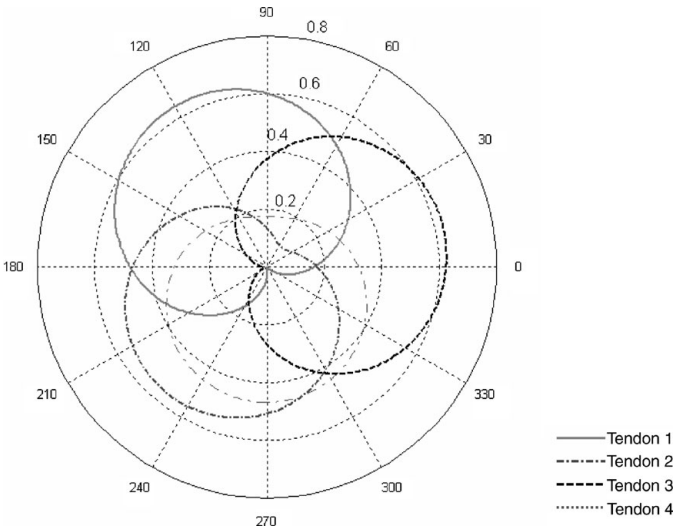


Fig. 8. Tendon forces (Newton) in structure No. (c), evaluated at isotropic posture.

https://doi.org/10.1017/S0263574709005475 Published online by Cambridge University Press

Table IV. List of maximum tendon forces at different positions.

No.	Maximal tendon force (Newton) (at given posture)	Maximal tendon force (Newton) (throughout the workspace)
a	[0.6064 0.6063 0.6063]	[0.6352 0.8888 0.9511]
b	[0.6928 0.6929 0.6929]	[1.0591 0.7154 1.1758]
c	[0.6417 0.5580 0.6292 0.4679]	[0.6717 0.8555 0.9797 0.5227]
d	[0.6425 0.5808 0.6275 0.4284]	[0.6726 0.8937 0.9625 0.4684]

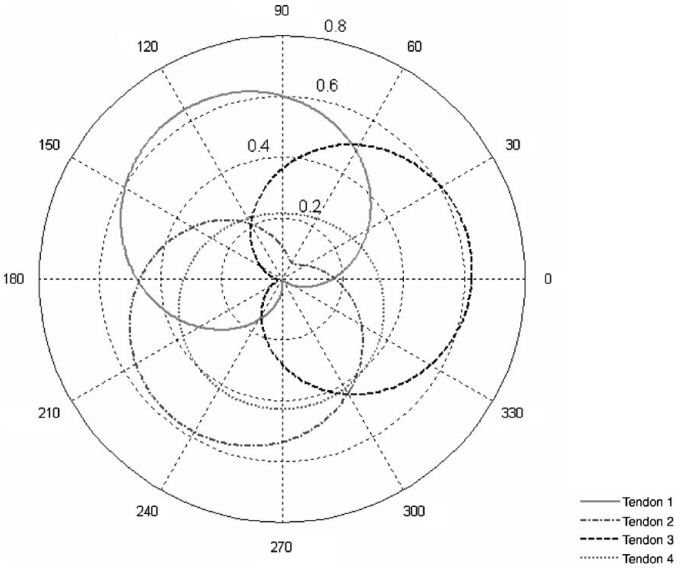


Fig. 9. Tendon forces (Newton) in structure No. (d), evaluated at isotropic posture.

positions for these four structure matrices. It can be observed that both maximum tendon forces at the isotropic posture and whole positions of No. (a) are smaller than those of No. (b). It can also be noted that information about the power required to control the tendon-driven manipulators can be obtained from these figures and Table IV.

6. Conclusion

Different tendon routings affect the force transmission in tendon-driven manipulators. In this work, the feasible tendon routing topology of a general n-DOF tendon-driven manipulator with m tendons is enumerated. The types of structure matrices can be further used as the atlas for the dimensional synthesis of tendon-driven manipulators. Design equations for the synthesis of tendon-driven manipulators with isotropic transmission characteristics are then developed via SVD method. The SVD method offers the designer a fast yet systematic means in determining the dimensions of tendon pulleys. Two examples of general structure matrices are used to demonstrate the methodology. It can be seen that this method provides designer with wider settings in determining the kinematic structures of tendon-driven manipulators with isotropic transmission characteristics. Although the isotropic transmission characteristics of a tendon-driven manipulator is position dependent, a better design of tendon-driven manipulators still can be achieved through careful selection of the tendon routing as well as the isotropic position.

Acknowledgements

The financial support from the National Science Council (NSC 95-2221-E-002-042-MY2) of Taiwan is gratefully acknowledged.

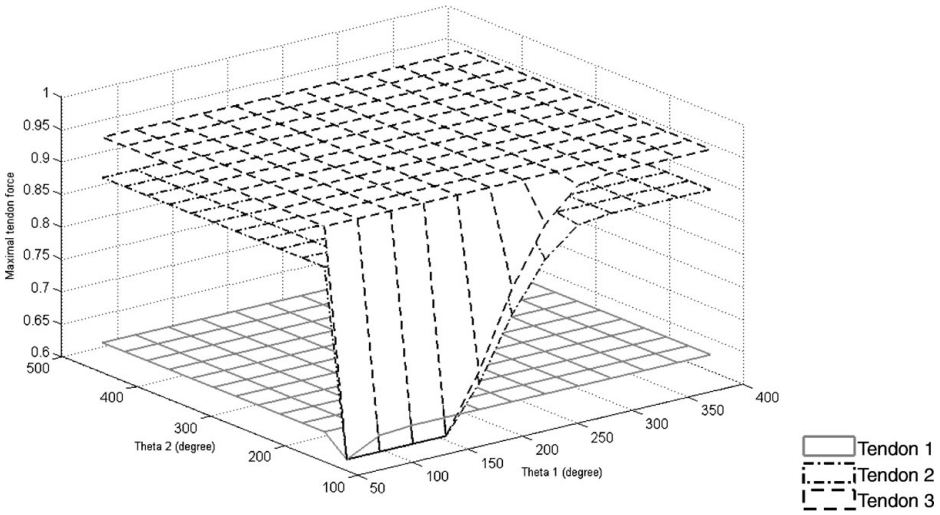


Fig. 10. Maximal tendon forces (Newton) of structure No. (a) throughout the workspace.

https://doi.org/10.1017/S0263574709005475 Published online by Cambridge University Press

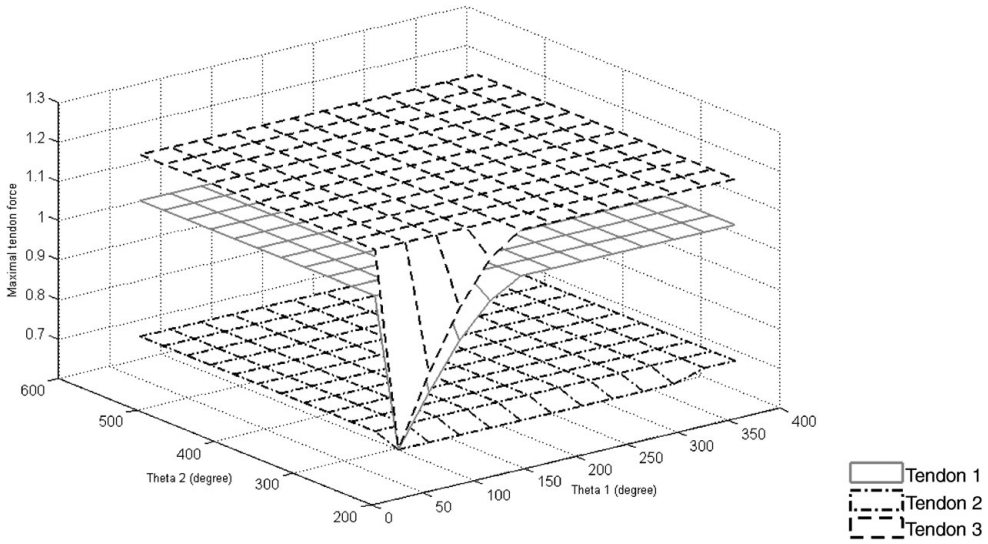


Fig. 11. Maximal tendon forces (Newton) of structure No. (b) throughout the workspace.

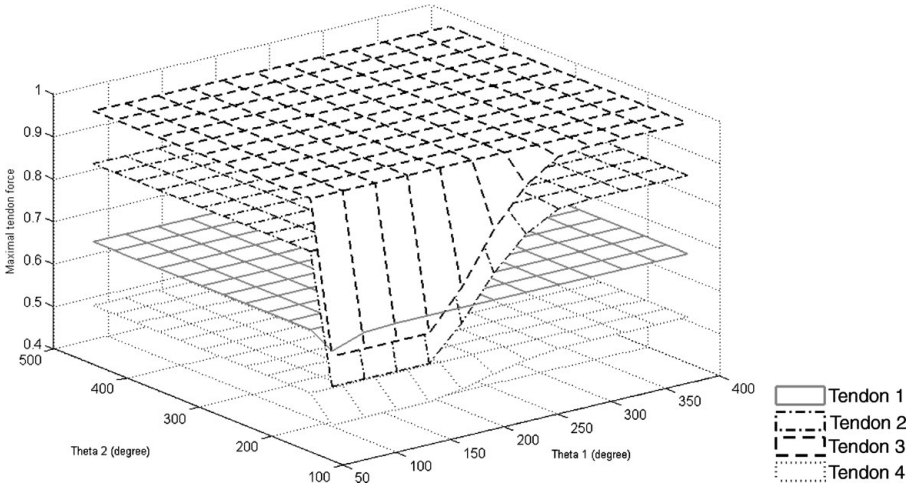


Fig. 12. Maximal tendon forces (Newton) of structure No. (c) throughout the workspace.

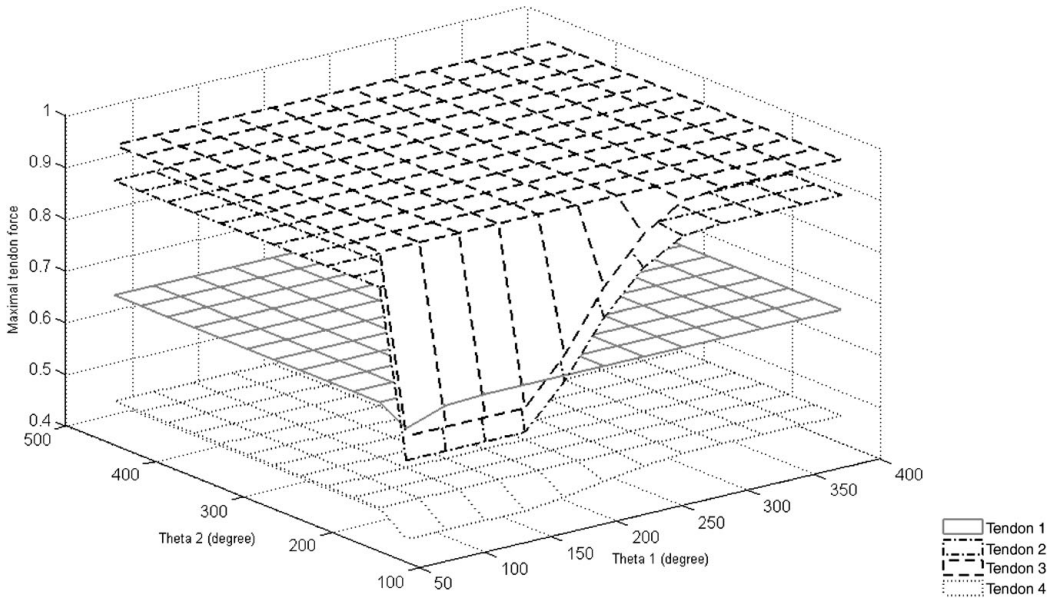


Fig. 13. Maximal tendon forces (Newton) of structure No. (d) throughout the workspace.

https://doi.org/10.1017/S0263574709005475 Published online by Cambridge University Press

References

1. A. Morecki, Z. Busko, H. Gasztold and K. Jaworek, "Synthesis and Control of the Anthropomorphic Two-Handed Manipulator," *Proceedings of 10th International Symposium on Industrial Robots*, Milan, Italy (1980) pp. 461–474.
2. J. K. Salisbury, Kinematic and Force Analysis of Articulated Hands *Ph.D. Dissertation* (Stanford, CA: Department of Mechanical Engineering, Stanford University, 1982).
3. L. W. Tsai and J. J. Lee, "Kinematic analysis of tendon-driven robotic mechanisms using graph theory," *ASME J. Mech. Trans. Automat. Des.* **111**(1), 59–65 (1989).
4. S. C. Jacobsen, H. Ko, E. K. Iversen and C. C. Davis, "Control strategies for tendon-driven manipulators," *IEEE Contr. Syst. Mag.* **10**(2), 23–28 (Feb. 1990).
5. M. G. Hollars and R. H. Cannon, "Initial Experiments on the End-point Control of A Two-link Manipulator with Flexible Tendons," *ASME Winter Annual Meeting*, Miami, FL (1985)
6. S. Oh, J. Ryu and K. Agrawal, "Dynamics and control of helicopters with a six-cables suspended robot," *ASME J. Mech. Des.* **128**, 1113–1121 (2006).
7. Y. H. Lee and J. J. Lee, "Modeling of the dynamics of tendon-driven robotic mechanisms with flexible tendons," *Mech. Mach. Theory* **38**(12), 1431–1447 (2003).
8. G. M. Prisco and M. Bergamasco, "Dynamic Modeling of a Class of Tendon Driven Manipulators," *Proceedings of IEEE International Conference on Robotics and Automation*, Monterey, CA (1997).
9. P. A. Voglewede and I. Ebert-Uphoff, "Application of the antipodal grasp theorem to cable-driven robots," *IEEE Trans. Rob.* **21**(4), 713–718 (2005).
10. G. Barrette and C. Gosselin, "Determination of the dynamic workspace of cable-driven planar parallel mechanisms," *ASME J. Mech. Des.* **127**(2), 242–248 (2005).
11. X. Diao and O. Ma, "A method of verifying the force-closure condition for general cable manipulators with seven cables," *Mech. Mach. Theory* **42**(12), 1563–1576 (2007).
12. Bar-Cohen, *Biomometics, Biologically Inspired Technologies* (CRC Press Taylor & Francis Group, FL, 2006) pp. 267–290.
13. Jyh-Jone Lee and Lung-Wen Tsai, "The structural synthesis of tendon-driven manipulators having a pseudotriangular structure matrix," *J. Rob. Res.* **10**(3), 255–262 (1991).
14. T. Yoshikawa, "Dynamic Manipulability of Robot Manipulators," *IEEE International Conference on Robotics and Automation. Proceedings* (Mar. 1985) pp. 1033–1038.
15. P. Chiacchio and M. Concilio, "The Dynamic Manipulability Ellipsoid for Redundant Manipulators," *Proceedings of IEEE International Conference on Robotics and Automation*, Leuven, Belgium (1998) pp. 95–100.
16. Jyh-Jone Lee and Lung-Wen Tsai, "Topological Analysis of Tendon-Driven Manipulators," *Eight World Congress on The Theory of Machines and Mechanism*, Prague, Czechoslovakia (Aug. 1991) pp. 479–482.
17. Yeong-Jeong Ou and Lung-Wen Tsai, "Kinematic synthesis of tendon-driven manipulators with isotropic transmission characteristics," *ASME J. Mech. Des.* **115** 884–891 (1993).
18. Dar-Zen Chen, Jiun-Chin Su and Kang-Li Yao, "A decomposition approach for the kinematic synthesis of tendon-driven manipulators," *J. Rob. Syst.* **16**(8), 433–443 (1999).
19. L. W. Tsai, *Robot Analysis—The Mechanics of Serial and Parallel Manipulators* (John Wiley & Sons, Inc., 1999).
20. Jyun-Jheng Huang, Structural Synthesis of Tendon-Driven Robotic Manipulators Using Singular Value Decomposition Method, *MS Thesis* (Taiwan: Department of Mechanical Engineering, National Taiwan University, 2007).
21. Steven J. Leon, *Linear Algebra with Applications*, 6th ed. (Prentice Hall, Inc., New Jersey, U.S.A. 2002).

https://doi.org/10.1017/S0263574709005475 Published online by Cambridge University Press